

Influence Of Fan Shroud On Noise Of Automobile Cooling Fan

Wu Hao^a, Chen Lingshan^a, Du Wei^a

(^aAutomotive Engineering College, Shanghai University Of Engineering Science, Shanghai 201600)

Corresponding Author: Wu Hao

Abstract: In order to reduce the noise of automotive cooling fan and improve the cooling efficiency, the influence of the fan shroud on the noise of the cooling fan was studied. In this study, the CFD simulations were performed on an cooling fan and fan shroud in the environment of a simulated automobile engine compartment. And a test rig has been designed, constructed and used to test the noise of the double-fans cooling module using three different fan shroud structures. Results indicate the noise of fan with the banner-annular shroud is 1.98dB smaller than that of the model with the banner-shaped shroud. Furthermore, the different cross-sectional structure of the shroud makes different changes in the air flow. The shroud with simple structure won't not only reduce the disturbance of the air flow in the river basin, but will increase the number of vortices, add the disturbance, and improve the noise; The dense and regular structure of the shroud will make the air flow more stable and reduce noise.

Key Words: Double-fans module, Fan shroud structure, CFD Simulation, Fan noise, Sound pressure level

Date of Submission: 09-07-2018

Date of acceptance: 23-07-2018

I. INTRODUCTION

As one of the most important components of diesel locomotives and fuel cell vehicles, cooling fan plays a crucial role in the thermal management system [1-3]. The fan with high speed is beneficial to the vehicle's heat dissipation [4], however, its noise is also increased. Therefore, it is very meaningful to reduce the noise of the fan. The fan shroud is also an indispensable part of the cooling fan, which greatly influences the control of the cooling airflow of the vehicle [5,6]. Therefore, the research on the structure of the shroud is very valuable.

With respect to fan noise reduction, research should be conducted on noise sources. In recent years there have been many studies on the aerodynamic and acoustic performance of fans. The focus of this numerical analysis is on the impact of the tip-gap size on the overall flow field. In this study a reduction of the tip-gap width decreases the amplitude of the tip-gap vortex wandering and as such the region of influence of the turbulent wake and increases the frequencies of the dominant modes. Since this is confirmed, it also shows the dominant role of the tip-gap vortex in the noise emission [7]. Cattanei introduced the use of uneven circumferential blading pitch to reduce the effect of noise from axial rotors. They confirmed that make blading pitch uneven is an effective measure to reduce fan noise [8-10]. These above researches are aimed at the design of fan blade without investigating the structure of the cooling fan shroud.

Research on fan shroud at home and abroad, G Ren derived the fan shroud diameter and series-parallel connection have significant effects on the cooling module and resistance performance. The heat transfer performance can be enhanced by adjusting the diameter of the fan cover and changing the series-parallel connections [11]. N Karthikeyan studied that the performance characteristics of the forward and backward curved fans when put in to engine cowling and to compare flow delivered by the fans, and the result is that the cooling performance has been greatly improved after the improvement [12]. VK Srinivasa introduced the DoE method for optimization of cooling fan and fan shroud for automotive cooling systems [13]. LJ Gorny has been conducted a project to verify the efficacy of tunable resonators in reducing the tonal noise output from an industrial chiller's cooling fan. The primary goals of this work were to demonstrate resonator source robustness for attenuating blade tone noise generated by fixed speed fans, radiating primarily in a single direction, that have non-ideal, un-ducted flow conditions [14]. Jiao Guowang proposed to rationally design the shape of the cooling fan deflector of the loader, which can reduce the turbulence of the flow field and reduce the noise [15]. However, its research was only directed at the shroud itself without the fan. Sitaram measured the flow field at the rotor exit of a low aspect ratio axial flow fan for different tip geometries and for different flow coefficients. From steady state measurements, the performance of rotor with perforated partial shroud is found to be the best. Both the rotors with partial shrouds have stalled at a higher flow coefficient compared to that of rotor with partial shroud [16]. Edward Canepa proposed an experiment for the tip leakage noise generated by a shrouded rotor of an axial-flow fan. The measurements was taken at high flow rate and at the design point in a hemi-anechoic chamber, at constant rotational speed and during speed ramps. The results show the broadband part of the spectra and the peaks related to the tip leakage flow are affected by the same propagation effects, but show a

different dependence on the rotational speed and on the operating point. The upstream geometry affects the radiated noise much more than the performance and even a strong reduction in the tip leakage cannot completely eliminate the related noise [17]. Wang Dong studied the effect of the fan shroud on the cooling performance of the vehicle, and concluded that the larger angle of the transition section of the fan shroud, the smaller energy lost [18], but without in-depth study of its impact on noise. X Wang carried out an experimental and numerical investigation into the tip leakage flow of a turbine rotor, and through the validated turbulence model and numerical strategy, simulations are carried out to compare the characteristics of the tip leakage flow in three cases. The conclusion shows that the blade noise is influenced by the inaccurate viscous force arising from the stationary blade and shroud [19].

The fan shroud can effectively improve the air flow, but if its existence will have an impact on the noise, and what structure of the shroud has a great impact on the noise is the author's following work. This paper does the CFD simulation of the shroud by simulating the forecabin of the real car, and explore the influence of the fan shroud on fan noise in combination with specific experiments.

II. MATHEMATICAL MODEL OF THE FAN

1.1 Model building

First of all, it's essential to establish a three-dimensional model of the fan and the fan shroud. Fig.1 shows the automotive cooling fan and shroud model: Fig. 1a is the banner-shaped fan shroud; Fig. 1b is the banner-annular fan shroud; Fig. 1c is the banner-shaped fan shroud with blade; Fig. 1d is the banner-annular fan shroud with blade. Research object is a car cooling fan with 7 blades, whose outer diameter is 305mm, hub straight diameter is 115mm, hub ratio is 0.38, leaf thickness is 2mm, and mounting angle is 35°.

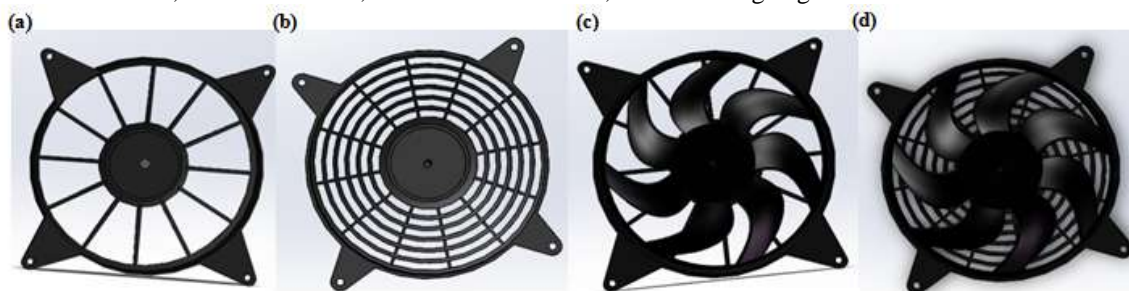


Fig. 1. Automotive cooling fan and shroud model, (a) the banner-shaped fan shroud, (b) the banner-annular fan shroud, (c) the banner-shaped fan, (d) the banner-annular fan.

1.2 Meshing

The CFD simulation are based on the FLUENT software [20], the fan model is meshed by the meshing software ICEM, then create the external flow field calculation domain, its diameter is 450mm, inlet is 200mm, outlet is 600mm. Because of the structure of the fan blade and the fan shroud is complex, it's reasonable to select the unstructured grid. At the same time, the way of the local mesh encryption of the fan blade makes the grid quality improve [21,22]. Then by setting the interface, the two interfaces perform Boolean operations and difference exchanges in the FLUENT software [23,24].

For the intra-channel flow calculation, the Realizable $k-\epsilon$ turbulence model can be selected. At the same time, an appropriate wall function must be selected to obtain accurate calculation results. Different wall functions require different boundary layer grids. The more common wall functions include the Standard Wall Functions, the Non-Equilibrium Wall Functions, the Scalable Wall Functions, and the Enhanced Wall Functions [25].

III. ANALYSIS OF SIMULATION

2.1 Flow field analysis of the cooling fan and its shroud

This paper simulates the three models of the banner-shaped fan shroud, the banner-annular fan shroud and no fan shroud. In the simulation, the turbulence model is selected as the calculation model, the SIMPLEC method is used for the force-velocity coupling [26], and the wall and fan shroud of the channel calculation domain were set as solid boundaries. At the same time, during the analysis of the flow field, local details such as holes and external ears are ignored to improve the computational efficiency [27].

The implicit solution of the split solver is used in the calculation of steady state, and chose the $k-\epsilon$ turbulence model [28].

As for the turbulent kinetic energy k equation:

$$\rho \frac{dk}{dt} = \frac{\partial}{\partial x_i} \left[\left(\mu_i + \frac{\mu_t}{\sigma_k} \right) \frac{\partial k}{\partial x_i} \right] + G_k + G_b - \rho \varepsilon \quad (1)$$

As for the turbulent dissipation rate equation:

$$\rho \frac{d\varepsilon}{dt} = \frac{\partial}{\partial x_i} \left[\left(\mu_i + \frac{\mu_t}{\sigma_\varepsilon} \right) \frac{\partial \varepsilon}{\partial x_i} \right] + C_\varepsilon \frac{\varepsilon}{k} (G_k + C_{3\varepsilon} G_b) - C_{2\varepsilon} \rho \frac{\varepsilon^2}{k} \quad (2)$$

In the above equations, μ_i is the laminar viscosity coefficient; $\mu_t = \rho C_\mu k^2 / \varepsilon$ is the turbulent viscosity coefficient; G_k is the turbulent kinetic energy; G_b is the buoyant turbulent kinetic energy.

On the other hand, the LES model is selected in the calculation of transients, and the governing equations for large eddy simulations can be got by the Navier-Stokes equations [29]:

$$\frac{\partial \rho}{\partial t} + u \frac{\partial \rho \bar{u}_i}{\partial x_i} = 0 \quad (3)$$

$$\frac{\partial}{\partial t} (\rho \bar{u}_i) + \frac{\partial}{\partial x_j} (\rho \bar{u}_i \bar{u}_j) = \frac{\partial}{\partial x_j} \left(\mu \frac{\partial \bar{u}_i}{\partial x_j} \right) - \frac{\partial \bar{p}}{\partial x_j} - \frac{\partial \tau_{ij}}{\partial x_j} \quad (4)$$

In the above formulas, ρ means density; t is time; u_i , u_j are the filtered speed components; μ is the turbulent viscosity coefficient; τ_{ij} represents sub-grid-scale stress, where the $\tau_{ij} = \rho \bar{u}_i \bar{u}_j - \rho \bar{u}_i \bar{u}_j$.

Above all, making analysis of the flow field of the cooling fan shroud, according to the vehicle cooling requirements, the flow rate is set to 21.2 m/s, in this simulation, and the outlet is set to outflow. Fig.2 shows simulation results of the fan shroud.

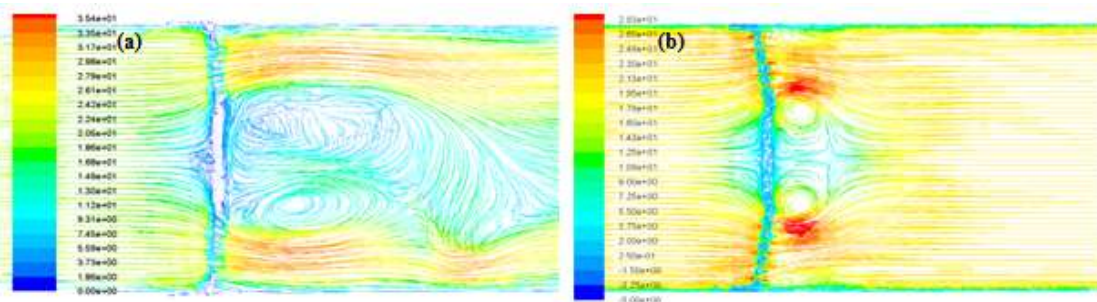


Fig. 2. Diagram of speed streamline, (a) speed streamline diagram of the banner-shaped fan shroud, (b) speed streamline diagram of the banner-annular fan shroud.

Fig. 2a shows the speed streamline diagram of the banner-shaped fan shroud, from where it can be observed that the flow rate at the outer edge of the basin is higher than the internal, moreover, the internal streamline is more chaotic; there are two large vortices behind the shroud, whose shape are irregular, in addition, at the end of the domain, more vortices is appearing.

Fig. 2b shows the speed streamline diagram of the banner-annular fan shroud, the flow rate at the outer edge of the basin is still higher, but comparing with the Fig. 2a, the streamline is more steady. On the other hand, there are two symmetrical vortices when the fluid passes through the shroud.

In the above two flow fields, there are two different eddy regions which are violent turbulences. After analysis, it can be inferred that these eddy regions are the aerodynamic noise sources of the fan shroud, moreover, the noise has the characteristics of dipole sound sources [30].

Then, after analyzed the influence of the fan shroud on the airflow, it is necessary to simulate the flow field and the noise of the fan shroud with fan blade in operation. Fig. 3 shows the streamline diagram of the cooling fan at 2700r/min; Fig. 4 shows the vortex diagram of the cooling fan at 2700r/min.

In case of the fan without shroud, Fig. 3a shows the streamline diagram, from where that the air flow in the flow field fluctuate slightly, and the fluctuations become more and more obvious from the inner edge to the outer edge; in Fig. 4a, it's obviously that there is more vortices at the outlet.

In case of the fan with the banner-shaped shroud, in Fig. 3b, the phenomenon of flow around the cylinder is obvious, and the flow fluctuated seriously, even the flow velocity is relatively low; as shown in Fig. 4b, the vortex is extremely turbulent, at the same time that there is vortices around the fan blades and the export.

In case of the fan with the banner-annular shroud, Fig. 3c shows the streamline diagram, from where that the river basin is relatively dense and stable with almost no fluctuations; as shown in Fig. 4c, the vortex is more regular.

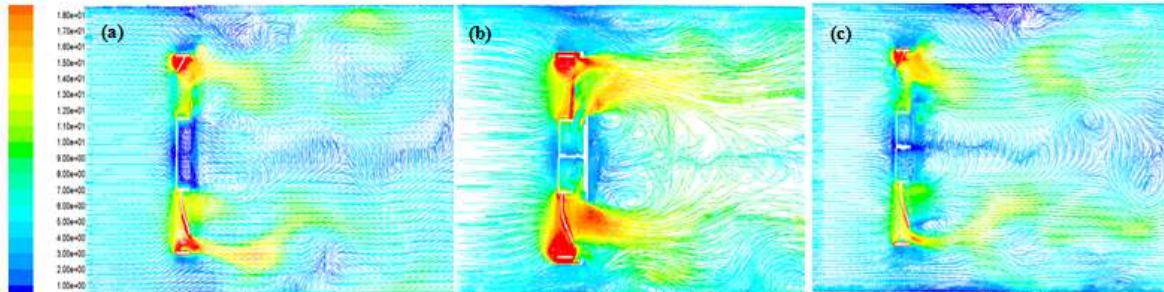


Fig. 3. The streamline diagram of the cooling fan at 2700r/min, (a) no fan shroud, (b) the banner-shaped fan shroud, (c) the banner-annular fan shroud.

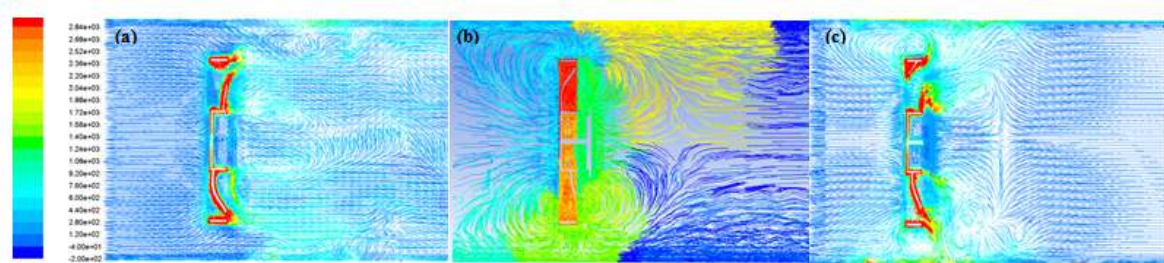


Fig. 4. The vortex diagram of the cooling fan at 2700r/min, (a) no fan shroud, (b) the banner-shaped fan shroud, (c) the banner-annular fan shroud.

2.2 Sound field analysis of the cooling fan and its shroud

In order to observe the spectrum characteristics of the cooling fan and the shroud, it is using the Fast Fourier Transform, make the pressure in time domain transformed into frequency domain [31], because it is easier and more intuitive to observe characteristics in the frequency domain and is easily implemented in the Fluent. As we all know, in the testing of acoustic signals, there is a common method is to convert the time domain signal into the frequency domain signal by the Fourier Transform of and its inverse transform.

At first, showing the Fourier Transform formula:

$$F(\omega) = \int_{-\infty}^{\infty} f(t) e^{-i\omega t} dt \quad (5)$$

Then, showing the inverse Fourier Transform formula:

$$f(t) = \frac{1}{2\pi} \int_{-\infty}^{\infty} F(\omega) e^{i\omega t} d\omega \quad (6)$$

It's not enough that if only get the frequency domain signal, it's important to convert the each point's pulsating pressure value measured in the simulation into a pulsating pressure level by the sound pressure level formula [32]. The formula is shown as follow.

$$SPL = 20 \lg \left(\frac{P_e}{P_r} \right) \quad (7)$$

In the above formula, P_e means the pulsating pressure; $P_r = 2 \times 10^{-5} Pa$ is reference the sound pressure.

Figs. 5, 6 and 7 are the pulsating pressure-level frequency domains of each monitoring point of the three models.

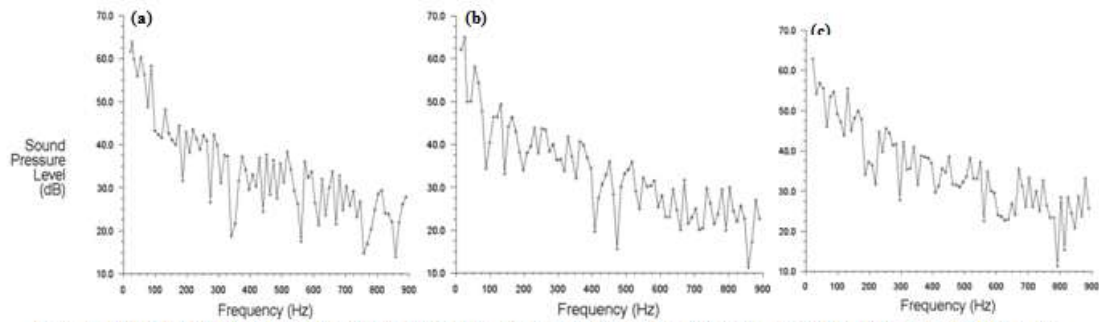


Fig. 5. The pulsating pressure level frequency domain of three monitoring points without fan shroud, (a) the data of the No. 1 monitoring point, (b) the data of the No. 2 monitoring point, (c) the data of the No. 3 monitoring point.

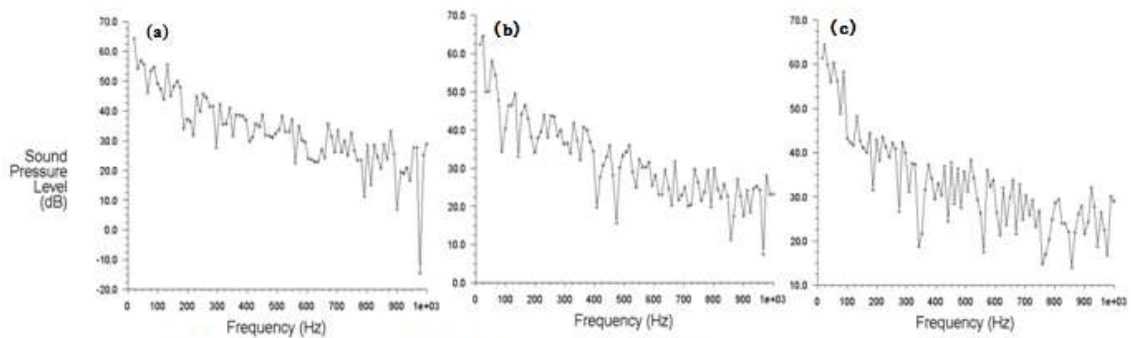


Fig. 6. The pulsating pressure level frequency domain of three monitoring points with the banner-shaped fan shroud, (a) the data of the No. 1 monitoring point, (b) the data of the No. 2 monitoring point, (c) the data of the No. 3 monitoring point.

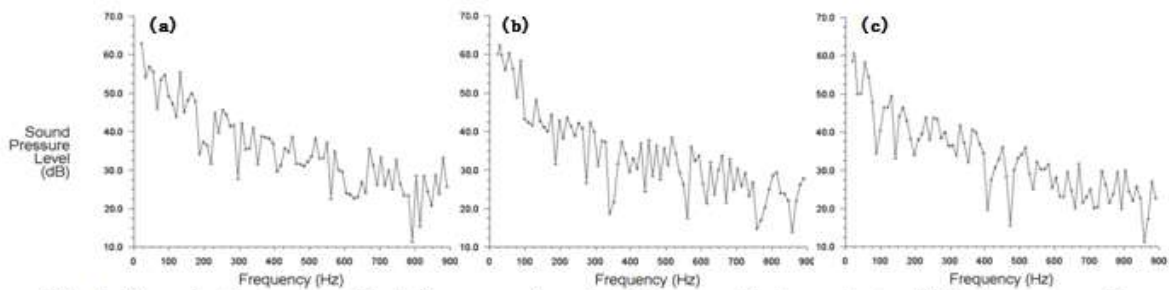


Fig. 7. The pulsating pressure level frequency domain of three monitoring points with the banner-annular fan shroud, (a) the data of the No. 1 monitoring point, (b) the data of the No. 2 monitoring point, (c) the data of the No. 3 monitoring point.

From the above series of sound pressure level frequency domain diagrams, it's observed that the band of each monitoring point's sound pressure level is very wide, the total sound pressure level is showing a decreasing trend as the frequency increase, its maximum energy is appearing in the low frequency, is approximately 40Hz. The most important result is that as the frequency increase, the point's amplitude is dropping. The sound pressure level of model A is approximately 64.20 dB; as for model B is about 65.06 dB; the model C is approximately 62.26 dB. The specific data is shown in Table 1.

By comparing the sound pressure levels of the models, it can be seen that although the amplitude is different at different frequency, the frequency domain diagram of the entire sound pressure level is similar and the trend of changing is similar.

Table 1 Sound pressure level values of various models and monitoring points

The model of fan shroud	Monitoring points	Sound pressure level /dB	Average sound pressure level /dB
A (No fan shroud)	NO.1	64.1	64.20
	NO.2	62.8	

	NO.3	63.2	
B (Banner-shaped fan shroud)	NO.1	64.8	65.06
	NO.2	65.1	
	NO.3	65.3	
C (Banner-annular fan shroud)	NO.1	62.6	62.26
	NO.2	62.5	
	NO.3	61.7	

IV. EXPERIMENTAL RESULT VERIFICATION

At the end of the page, we conduct the special noise test so as to verify the credibility of simulation. In the simulation, its calculating basin is designed at the size of the car's forecabin, which has a length of 1200mm, a width of 1000mm, and a height of 700mm. As for the text, which is conducted in a full anechoic room. Fig. 8a shows the layout of these acoustic sensors which are centered on a fan [33], in order to observe more intuitively; Fig. 8b shows the experimental rig. Before the experiment, the background noise should be measured [34], then get the value of 46.23dB.

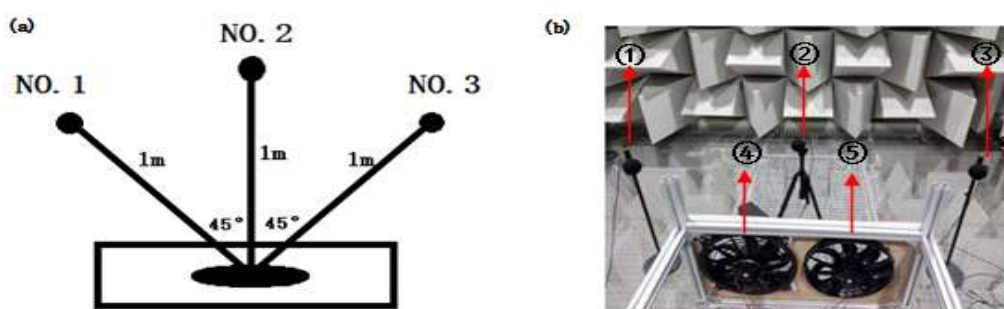


Fig.8. Experimental rig, (a) acoustic sensor layout diagram, (b) photo of the rig (1,3—acoustic sensors; 4—the fan with banner-annular fan shroud; 5—the fan with banner-shaped fan shroud)

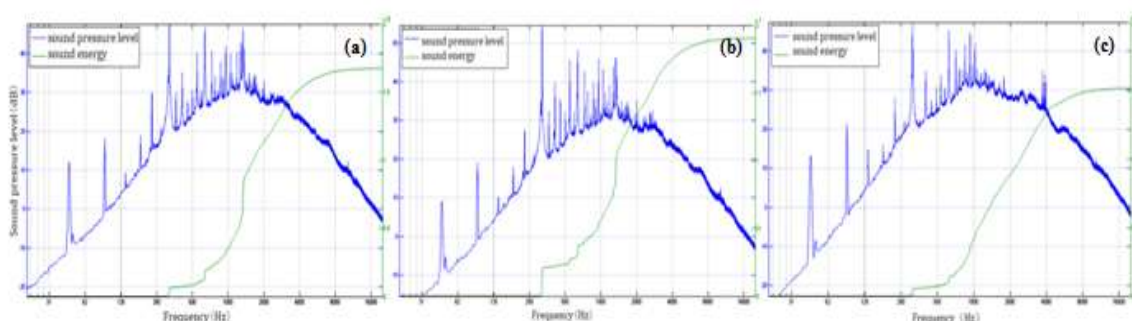


Fig. 9. The Noise Spectrum And Cumulative Energy Spectrum Of Each Fan Shroud Model, (A) No Fan Shroud, (B) The Banner-Shaped fan Shroud, (C) The Banner-Annular Fan Shroud.

In the following experiment, all the fans' speed is set at 2700r/min. In the case of no fan shroud, The first-order frequency of the fan is $2700\text{Hz}/60=45\text{Hz}$, as shown in Fig. 9a, from where it can be observed that at this speed, the noise is the maximum when the frequency is 315 Hz, which further proves that the maximum noise of the fan at high speed is the order noise corresponding to the number of fan blades, and the total sound pressure level is 66.02 dB.

In the case of the banner-shaped fan shroud, the main order noise appears at the 7th order of 315Hz, the 12th order of 541Hz and the 14th order of 630Hz. As shown in Fig. 9b, obviously, that the maximum noise still appears at 315Hz. After the calculation, the sound pressure level is 66.78dB.

In the case of the banner-annular fan shroud, as shown in Fig. 9c, it test the lowest sound pressure level about 64.80dB.

Table 2 shows the comparison of models' simulated data and experimental data, from where that the noise of each model in the experiment is higher than it in the simulation. After analysis, the simulation's environment is better than the experiment's, and the quality of the grid model make deviations between the simulation data and the experimental data, however, the error is within the acceptable range. Ultimately, the results

of the experiment agree well with the results of the simulation analysis, that is the fan with the banner-shaped shroud have the maximum sound pressure level, while the fan with the banner-annular fan shroud have the minimal sound pressure level.

Table 2 Comparison of models' simulated data and experimental data

the model of fan shroud	Simulated data /dB	Experimental data /dB	Deviation/dB
A(No fan shroud)	64.20	66.02	1.82
B(Banner-shaped shroud)	65.06	66.78	1.72
C(Banner-annularshroud)	62.26	64.80	2.54

V. CONCLUSIONS

In this paper, numerical simulation and experimental method are used to study the effect of fan shroud on automotive cooling fan's noise. The main results are as follows:

(1) This experiment is to verify the noise value relationship of the shroud in the simulation, in addition, the maximum noise is belong to the fan with the banner-shaped shroud, the minimum noise is created by the model with the banner-annularshroud, moreover, the noise of fan with the banner-annularshroud is 1.98dB smaller than that of the model with the banner-shaped shroud. As for the diagram, it's obvious that these curves change similarly, and the amplitude appears in the low frequency area is about 45 Hz.

(2) The cross-sectional shape of the three fan shrouds are different, when airflow go through the fan shroud can be changed due to its position and deflection angles. The shroud with simple structure won't not only reduce the disturbance of the air flow in the river basin, but will increase the number of vorticities, add the disturbance; The dense and regular structure of the shroud will make the air flow more stable.

(3) The fan's noise is related to the stability of the flow field, the more stable flow field is, the less vortices there is and the smaller fan's noise will be. Without affecting the fan flow, the structure of the fan shroud is more dense and the noise is smaller.

REFERENCES

- [1]. G Zhang, SG Kandlikar. A critical review of cooling techniques in proton exchange membrane fuel cell stacks. *International Journal of Hydrogen Energy*. 2012, 37(3): 2412-2429.
- [2]. C Xiao, Q Tian, C Zhou et al. A novel cooling system based on heat pipe with fan for thermal management of high-power LEDs. *Journal of Optics*. 2016, 46(3): 1-8.
- [3]. HC Su, CL Liu, TJ Pan et al. Investigation of a multiple-vibrating fan system for electronics cooling. *Semiconductor Thermal Measurement & Management*. 2013: 110-115.
- [4]. A Colmenar-Santos, L Alberdi-Jiménez, L Nasarre-Cortés, J Mora-Larramona. Residual heat use generated by a 12kW fuel cell in an electric vehicle heating system. *Energy*. 2014, 68 (8): 182-190.
- [5]. G Ren, S Heo, TH Kim, C Cheong. Response surface method-based optimization of the shroud of an axial cooling fan for high performance and low noise. *Journal of Mechanical Science & Technology*. 2013, 27(1): 33-42.
- [6]. M Khaled, F Mangi, HE Hage, F Harambat, H Peerhossaini. Fan air flow analysis and heat transfer enhancement of vehicle underhood cooling system – Towards a new control approach for fuel consumption reduction. *Applied Energy*. 2012, 91(1): 439-450.
- [7]. A Pogorelov, M Meinke, W Schröder. Effects of tip-gap width on the flow field in an axial fan. *International Journal of Heat & Fluid Flow*. 2016, 61.
- [8]. Cattanei A, Ghio R, Bongiovi` A. Reduction of the tonal noise annoyance of axial flow fans by means of optimal blade spacing. *Applied Acoustics*. 2007, 68(11-12): 1323-1345.
- [9]. E Canepa, A Cattanei, FM Zecchin. Analysis of tonal noise generating mechanisms in low-speed axial-flow fans. *Journal of Thermal Science*. 2016, 25(4): 302-311.
- [10]. E Canepa, A Cattanei, FM Zecchin. Effect of the rotor-stator gap variation on the tonal noise generated by axial-flow fans[J]. *Applied Acoustics*. 2015, 94: 29-38.
- [11]. G Ren, S Heo, TH Kim, C Cheong. Response surface method-based optimization of the shroud of an axial cooling fan for high performance and low noise. *Journal of Mechanical Science & Technology*. 2013, 27(1): 33-42.
- [12]. N Karthikeyan, A Gokhale, A Shinde. Optimization of power consumed by scooter engine cooling fan. *SAE International Journal of Engines*. 2013, 6(1): 1-9.
- [13]. VK Srinivasa, S Renjith, B Shome. Design of experiments enabled CFD approach for optimizing cooling fan performance. *Sae World Congress*. 2014, 1.
- [14]. LJ Gorny, GH Koopmann. A true to life application for flow driven resonators: Industrial chiller cooling fan noise reduction. *Journal of the Acoustical Society of America*. 2010, 127(3): 1767.
- [15]. Jiao Guowang, Zhang Jianrun, Li Hongwei. The scheme of aerodynamic noise analysis and noise reduction for loader's cooling fan shroud. *Construction Machinery and Equipment*. 2010, 41(3): 46-49.
- [16]. N Sitaram, GCV Sivakumar. Effect of partial shrouds on the performance and flow field of a low-aspect-ratio axial-flow fan rotor[J]. *International Journal of Rotating Machinery*. 2011(1023-621X).
- [17]. Edward Canepa, Andrea Cattanei, Fabio Mazzocut Zecchin et al. An experimental investigation on the tip leakage noise in axial-flow fans with rotating shroud. *Journal of Sound and Vibration*. 2016, 4(9): 115-131.
- [18]. Wang Dong, Huang Xiao, Xiao Lu. Influence of fan cowl on automotive cooling module performance. *Journal of Jiangsu University(Natural Science Edition)*. 2017, 38(3): 260-266.
- [19]. X Wang, J Wang, F He, H Zhang. Effect of Relative Movement between the Shroud and Blade on Tip Leakage Flow Characteristics. *Energies*. 2017, 10(10): 1600.
- [20]. M Mehravaran, Y Zhang. Optimizing the geometry of fan-shroud assembly using CFD. *Sae Technical Papers*. 2015, 3(8): 25-37.
- [21]. N Kang, Y Cao. Research on computational fluid dynamics with effect of grid quality on the accuracy of simulated results of two dimensional low-speed parallel flow. *Applied Mechanics & Materials*. 2014, 685: 232-235.

- [22]. D Toris, C Rogsch, A Seyfried. Usefulness of finer grid to increase the approximation quality of LES-based CFD-calculations related to buoyancy-driven flows. *Botanica Marina*. 2007, 38(8):513-518.
- [23]. DQ Xue, DY Lv, JX Zhang, SL Hou. The Optimization on Grid Division Methods of Blade Pump Blades Based on CFD. *Applied Mechanics & Materials*. 2014, 635-637:35-39.
- [24]. S Rane, A Kovacevic, N Stosic, M Kethidi. Deforming grid generation and CFD analysis of variable geometry screw compressors. *Computers & Fluids*. 2014, 99(5):124-141.
- [25]. H Xie, S Zhang, X Guan. Effects of Turbulence Models and Wall Functions on the Numerical Simulation of Indoor Air Flow. *Journal of University of Shanghai for Science*. 2017, 39(1):81-85.
- [26]. A Toffolo, A Lazzaretto, AD Martegani. Cross-flow fan design guidelines for multi-objective performance optimization[J]. *Proceedings of the Institution of Mechanical Engineers Part A Journal of Power & Energy*. 2004, 218(1):33-42.
- [27]. X Zhang, P Zhang, L Zhang. A simple technique to improve computational efficiency of meshless methods[J]. *Procedia Engineering*. 2012, 31:1102-1107.
- [28]. JC Kok. Resolving the dependence on freestream values for the k-turbulence model. *Aiaa Journal*. 2012, 38(7):1292-1295.
- [29]. Raymond, Jean-Pierre, Thevenet, Laetitia. Boundary feedback stabilization of the two dimensional Navier-Stokes equations with finite dimensional controllers. *Discrete & Continuous Dynamical Systems*. 2012, 27(3):1159-1187.
- [30]. Li Hui, Xiao Xinbiao, Zhu Minhao. Analysis on aerodynamic noise in inter-coach space of high-speed train. *Journal of Vibration and Shock*. 2016, 35(6):109-114.
- [31]. Patanker S. V, Spalding D. B. A calculation procedure for heat, mass and momentum transfer in three-dimensional parabolic. *Int J Heat mass Transfer*. 1972, 15(10):1787-1806.
- [32]. T Lippert, M Galindo-Romero, AN Gavrilov, OV Estorff. Empirical estimation of peak pressure level from sound exposure level. Part II: Offshore impact pile driving noise. *Journal of the Acoustical Society of America*. 2015, 138(3):EL287.
- [33]. HH Heller. Acoustic sensor configuration for minimum flow noise generation. *Journal of the Acoustical Society of America*. 2005, 48(4):856-856.
- [34]. S Choi, Z Jiang. Comparison of envelope extraction algorithms for cardiac sound signal segmentation. *Expert Systems with Applications*. 2008, 34(2):1056-1069.

Wu Hao "Influence Of Fan Shroud On Noise Of Automobile Cooling Fan" *International Journal of Research in Engineering and Science (IJRES)*, vol. 06, no. 06, 2018, pp. 36-43.